We are IntechOpen, the world's leading publisher of Open Access books
Built by scientists, for scientists

6,100
Open access books available

167,000
International authors and editors

185M
Downloads

Our authors are among the

154
Countries delivered to

TOP 1%
most cited scientists

12.2%
Contributors from top 500 universities

CLARIVATE ANALYTICS
BOOK CITATION INDEX
INDEXED

WEB OF SCIENCE™

Selection of our books indexed in the Book Citation Index in Web of Science™ Core Collection (BKCI)

Interested in publishing with us?
Contact book.department@intechopen.com

Numbers displayed above are based on latest data collected.
For more information visit www.intechopen.com

Chapter 7

Ultra Wideband Transient Scattering and Its Applications to Automated Target Recognition

Hoi-Shun Lui, Faisal Aldhubaib, Stuart Crozier and Nicholas V. Shuley

Additional information is available at the end of the chapter

http://dx.doi.org/10.5772/intechopen.75059

Abstract

Reliable radar target recognition has long been the holy grail of electromagnetic sensors. Target recognition based on the singularity expansion method (SEM) uses a time-domain electromagnetic signature and has been well studied over the last few decades. The SEM describes the late time period of the transient target signature as a sum of damped exponentials with natural resonant frequencies (NRFs). The aspect-independent and purely target geometry and material-dependent nature of the NRF set make it an excellent feature set for target characterization. In this chapter, we aim to review the background and the state of the art of resonance-based target recognition. The theoretical framework of SEM is introduced, followed by signal processing techniques that retrieve the target-dependent NRFs embedded in the transient electromagnetic target signatures. The extinction pulse, a well-known target recognition technique, is discussed. This chapter covers recent developments in using a polarimetric signature for target recognition, as well as using NRFs for subsurface sensing applications. The chapter concludes with some highlights of the ongoing challenges in the field.

Keywords: radar target recognition, ultra wideband radar, transient electromagnetic scattering, singularity expansion method

1. Introduction

The need to quickly and accurately identify enemies in confrontational situations is essential to most defense applications. Such decisions often rely upon radar target recognition. The two primary functions of radar are inherent in the acronym, whose letters stand for radio detection and ranging. There are two main categories of radar target recognition techniques: imaging

IntechOpen

© 2018 The Author(s). Licensee IntechOpen. This chapter is distributed under the terms of the Creative Commons Attribution License (http://creativecommons.org/licenses/by/3.0), which permits unrestricted use, distribution, and reproduction in any medium, provided the original work is properly cited. CC BY

and what is termed signature recognition. Imaging radars provide a visualization of the target using techniques such as focus spot scanning and inverse synthetic aperture [1]. Signature recognition radar extracts some characteristics or a feature set that characterizes the target. Some of the techniques, such as radar cross section (RCS) [2], polarization techniques [3], high-resolution range profiles (HRRP) [4], scattering centers [5], and multiple frequency measurements [6], are all under this category. The main drawback of these techniques is that the extracted parameters usually vary with incident aspect. For most radar target recognition problems, usually, the incident aspect angles of the target are not known a priori. It is, therefore, preferable to implement a technique that is purely dependent on the target itself and independent of its aspect to the radar.

One of the methods that overcome the aspet-dependent limitation is termed resonance-based target recognition [7]. As the name states, resonance-based target recognition essentially characterizes the radar target based on the natural resonant frequencies (NRFs) embedded in the target response. These NRFs are purely dependent on the physical attributes of the radar target, i.e., its dielectric properties and physical geometry, and these parameters are independent on the incident aspect [7] and incident polarization states [8]. Provided of course the resonances are well excited, the feasibility of using the NRFs for target recognition has been successfully demonstrated in the literature [9–11].

This chapter aims to provide an overview of the fundamentals and the development of resonance-based target recognition. We commence the chapter with a short discussion on RCS—a well-known frequency-domain method on how electromagnetic scattering is characterized at microwave frequencies. The singularity expansion method (SEM), which is the theoretical framework for resonance-based target recognition, provides the physical description of the transient scattering phenomena in time and frequency domains. Technical solutions for retrieving the target-dependent NRFs from the transient target signatures and automated target recognition (ATR) algorithms will be covered. The recent development including the prospect of using full polarimetric signatures, as well as the potential use of the techniques in other sensing applications, is also discussed. Comments and suggestions for future development are considered in conclusion.

2. Resonance-based target recognition

RCS is a well-known technique to characterize target from 3 MHz up to 300 MHz (HF to mm) [2]. Attempts have also been made to perform RCS measurement in the terahertz frequency region [12, 13]. RCS is a measure of the power that is returned or scattered in a given direction, normalized with respect to the power of the incident field. Mathematically, the RCS (σ) of a target is defined as [2]

$$\sigma = 4\pi \lim_{R\to\infty} R^2 \frac{|\mathbf{E_s}|}{|\mathbf{E_i}|}, \tag{1}$$

where R is the range from the radar to the target and E_i and E_s are the amplitudes of the incident electric field from the radar transmitter and the scattered electric field from the target,

respectively. The scattered field and thus the RCS of a definitive target, in general, vary as a function of incident aspects, receiving aspects, and excitation frequency. In the resonant regime which the wavelength of illumination (λ) and the target size (L) are comparable ($0.4\lambda \leq L \leq 10\lambda$), every part of the target affects every other parts. The total field of any part of the target is the vectorial sum of the incident and scattered field due to every part of the scattering body. This collective interaction determines the overall electromagnetic current induced on the target, which explains why the induced current at resonant frequencies is dependent on the physical attributes of the target.

Resonance-based target recognition is based on the resonating electromagnetic current induced on the target such that the ratio of excitation wavelength (λ) and the target size (L) has to be within the resonance scattering regime. The induced current serves as a secondary source and reradiates such that the resonant modes are embedded in the scattered target response. Rather than a frequency-domain characterization using RCS, one can also illuminate the target at a particular aspect in the time domain through a short-pulse excitation, measure the corresponding transient response at the same position (monostatic) or any another aspect (bistatic), and obtain the impulse response of the target. If one applies a Fourier transform to the target impulse response, this is the same as obtaining the frequency-domain "transfer function" of the target, thus evaluating the frequency dependency of the RCS at a particular transmit-receive configuration. Indeed, we assume that the bandwidth of the pulse is wide enough such that it covers at least the first few dominant resonant frequencies of the target.

2.1. Singularity expansion method

In the context of linear time-invariant (LTI) systems, the impulse response characterizes the behavior of the system and circuit. In the mid-1960s, Kennaugh and Moffatt [14] extended the concept of the impulse response and applied it to transient electromagnetic scattering from definitive targets. In the early 1970s, Baum [7] introduced the SEM that describes transient scattering phenomena. According to SEM, the entire transient target signature can be divided into two parts, namely, the early time and the late time period. Conceptually, the early time period is defined as the period from when the electromagnetic pulse initially strikes the target until the target is fully illuminated, while the commencement of the late time period is the time when global resonance has been fully established and the excitation is no longer present.

In the early time, the target is partly illuminated such that the majority of the scattering events originate locally from different parts of the target: specular reflections, diffraction from non-planar surfaces, edges, and corners. The occurrence of these events depends on when the pulse strikes on these edges and corners, and thus these early events are local, aspect dependent, and polarization dependent. They can be individually treated as scattering centers [5] or more generally using a wavefront description [15]. In the time domain, these scattering events correspond to impulse-like components, and they are time-varying (nonstationary) and can be modeled in a circuit context using an entire function [7, 16, 17].

In contrast, the commencement of the late time period is the time when the target is fully illuminated such that resonant modes at distinct frequencies are fully established. As previously mentioned the total field at any part of the target is a collective interaction of the incident

and scattered field from every single part of the target. At particular frequencies, the induced current on the target is freely resonating, and resonant modes are established. These resonant modes, known as natural resonance frequencies (NRFs), are theoretically dependent only on the physical attributes of the target and are independent of the aspect [7] and polarization [8]. This allows them to be an excellent candidate to be used as a feature set for target classification. Mathematically, the late time target signature can be modeled as a sum of damped exponentials with constant residues, i.e.,

$$r(t) = \sum_{n=1}^{N} \left[A_n e^{s_n t} + A_n^* e^{s_n^* t} \right], \quad t > T_l \tag{2}$$

where N is the modal order of the signal—the number of modes embedded in the late time response. It is assumed that only N modes are excited given that the pulse excitation is band-limited. T_l is the onset of the late time and * denotes the complex conjugate. A_n is the aspect-dependent residues. $s_n = \sigma_n \pm j\omega_n$ is the complex NRF. $\sigma_n (< 0)$and ω_n are the damping coefficients and resonant frequencies of the n^{th} mode, respectively.

2.2. Resonance extractions for target classification

Target classification and recognition rely on accurate extraction of the target-dependent NRFs. There are two main approaches to extract these NRFs. The first one is based on the mathematical formulation of the scattering problem. Through a Fourier transform, the short-pulse excitation corresponds to a broadband of frequencies in the frequency domain. If we formulate the entire scattering problem at a particular frequency via an integral equation formulation, the integral equation relationship can be written in a matrix form and solved via moment methods [18]. In general, this can be written as

$$[\mathbf{Z}][\mathbf{I}] = [\mathbf{V}], \tag{3}$$

where $[\mathbf{Z}]$ is an impedance-like matrix corresponding to the target geometry and $[\mathbf{I}]$ and $[\mathbf{V}]$ are column vectors corresponding to the unknown current induced on the target and the excitation, respectively. The natural resonant modes of the target, $s_n = \sigma_n \pm j\omega_n$, are those such that the homogenous version of Eq. (3) has a nontrivial solution. This implies that the solution exists when the determinant of the $[\mathbf{Z}]$ matrix equals zero, thus establishing the singularities of the $[\mathbf{Z}]$ matrix. These singularities can be extracted using a typical (complex) root searching method such as Muller's method [7]. The $[\mathbf{Z}]$ matrix is constructed based solely on the geometry and dielectric properties of the target. The NRFs are therefore totally independent of the incident aspect angle. A major limitation is that the entire physical problem needs to be modeled using moment method, and each $[\mathbf{Z}]$ corresponds to only one frequency. This means that one needs to repeat the entire root searching process for all the frequency points, which requires extensive computation. Another limitation is that this method cannot be applied directly to measured data.

Shortly after the proposition of SEM by Baum, Van Blaricum and Mittra [19] proposed using Prony's method which directly retrieves the NRFs and residues from the late time response in

a computationally affordable manner. Prony's method addresses the above limitations, and it has drawn significant attention in the field. However, the primary drawback of Prony's method is that the accuracies of the extracted parameters are highly sensitive to noise and the estimated modal order of the signal. Since then, many techniques have been proposed which can accurately retrieve the modal order, NRFs, and residues with noisy target signatures. To date, direct extraction of NRFs from late time target signature has become the principal approach in this context, and matrix pencil methods (MPM) developed by Sarkar and Pereira [20] have become the main tool for this purpose.

To illustrate how NRFs can be used for target classification, as well as the aspect dependency nature of the resides, an example of a 1 m wire target illuminated under different excitation aspect angles θ shown in **Figure 1** is considered [21]. The wire target of length (ℓ) and radius (a) ratio $\ell/a = 200$ is excited by a plane wave with the electric field in the plane of the wire. The transient target responses are obtained using the indirect time-domain method [22]—the scattering problem is first solved in the frequency domain at a large number of discrete frequency points, followed by Gaussian windowing to model a Gaussian pulse excitation [23] and an inverse Fourier transform. Here, the electromagnetic problem is solved using the moment method solver FEKO [24] from 4.39 MHz to 9 GHz with 2048 equally spaced samples. Given the target and incident aspect angles to the target, the late time can be approximated by

$$T_l = T_b + T_p + 2T_{tr}, \tag{4}$$

where T_{tr} is the maximal transit time of the target, T_p is the effective pulse duration, and T_b is the estimated edge when the pulse strikes the leading edge of the target [11]. The Gaussian pulse commences at $T_b = 10ns$ with $T_p = 0.22ns$. According to the geometry of **Figure 1**, $T_{tr} = \ell\cos\theta/c$ where $c = 3 \times 10^8 m/s$, and the excitation angles of $\theta = 15^\circ$, 45° and 75° are considered, resulting in $T_l \approx 16.6$ns, 14.92ns and 11.9ns, respectively. The NRFs are extracted using the MPM [20] with late time samples from 17 to 140 ns. The first ten dominant extracted NRFs are listed in **Table 1** and are compared with the ground truth—NRFs extracted using a root searching procedure of the [**Z**] matrix [25].

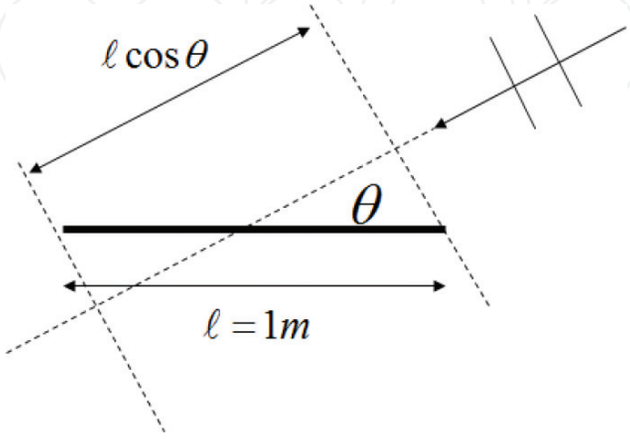

Figure 1. The wire scatterer with plane wave incidence (reprinted from [21] with permission from IEEE).

The results show that all the first ten dominant resonant modes can be extracted only at $\theta = 15^{\circ}$, while some modes cannot be retrieved at $\theta = 45^{\circ}$ and $\theta = 75^{\circ}$. To investigate of what is happening as the incidence angle varies, we transform the transient signatures to the joint time-frequency (TF) domain such that the existence and occurrences of the NRFs and scattering phenomena are clearly observed. Of all the time-frequency distributions (TFDs) in the Cohen class and the reassigned TFDs [26, 27], the Smooth Pseudo Wigner-Ville Distribution (SPWVD) gives reasonable TF resolutions without introducing uninterpretable artifacts [28–30].

The SPWVD, together with the corresponding time and frequency responses of the three signals, is shown in **Figure 2(a)–(c)**. At $\theta = 15^{\circ}$, all the ten modes are identified in the joint TF domain. In **Figure 2(b)**, modes 1 to 5 and mode 9 are observed when the incident angle is changed to 45°. Mode 6 is not observed due to its small residue. Two resonant modes at about 1.2 and 1.5 GHz are also found in the figure. They have similar frequencies to modes 8 and 10 but with higher damping factors (marked with ^ in **Table 1**), which could probably be the higher layer NRFs [31]. As the incident angle changes to 75°, only modes 1 to 4, 6, 7, and 9 are excited, and they are be found correspondingly to those frequencies in **Figure 2(c)**. In addition to the TF results, the NRFs also appear as peaks in the frequency response. As shown in both TF and frequency domains, it is apparent that the strength of the resonant modes, i.e., the residues, changes as the incident aspect varies, which validates the aspect dependency nature of the residues.

2.3. Extinction pulse technique

The target-dependent nature of the NRFs implies that the NRF patterns appearing in the S-plane are unique for a given target. Target recognition can thus be easily achieved by visually inspecting the patterns of the NRFs in the S-plane [32]. To automate the identification

n	f (MHz)	$[\mathbf{Z}]$ [25]	Matrix pencil method [20]		
		s_nL/c	15°, s_nL/c	45°, s_nL/c	75°, s_nL/c
1	138	$-0.260 \pm j2.91$	$-0.252 \pm j2.87$	$-0.253 \pm j2.87$	$-0.252 \pm j2.87$
2	286	$-0.381 \pm j6.01$	$-0.372 \pm j5.93$	$-0.370 \pm j5.93$	$-0.373 \pm j5.93$
3	432	$-0.468 \pm j9.06$	$-0.455 \pm j9.01$	$-0.458 \pm j9.01$	$-0.444 \pm j9.05$
4	583	$-0.538 \pm j12.2$	$-0.525 \pm j12.1$	$-0.512 \pm j12.1$	$-0.545 \pm j12.1$
5	730	$-0.600 \pm j15.3$	$-0.585 \pm j15.2$	$-0.609 \pm j15.2$	
6	879	$-0.654 \pm j18.4$	$-0.637 \pm j18.3$	$-0.833 \pm j18.4$	$-0.881 \pm j17.6$
7	1027	$-0.704 \pm j21.5$	$-0.692 \pm j21.4$		$-0.850 \pm j21.6$
8	1175	$-0.749 \pm j24.6$	$-0.733 \pm j24.6$	$-1.043 \pm j24.5$^	
9	1323	$-0.792 \pm j27.7$	$-0.785 \pm j27.7$	$-0.732 \pm j27.9$	$-1.005 \pm j28.6$
10	1471	$-0.832 \pm j30.8$	$-0.817 \pm j30.8$	$-1.294 \pm j30.9$^	

Table 1. Comparison between the extracted NRFs (s_nL/c) using $[\mathbf{Z}]$ matrix and MPM (reprinted from [21] with permission from IEEE).

http://dx.doi.org/10.5772/intechopen.75059

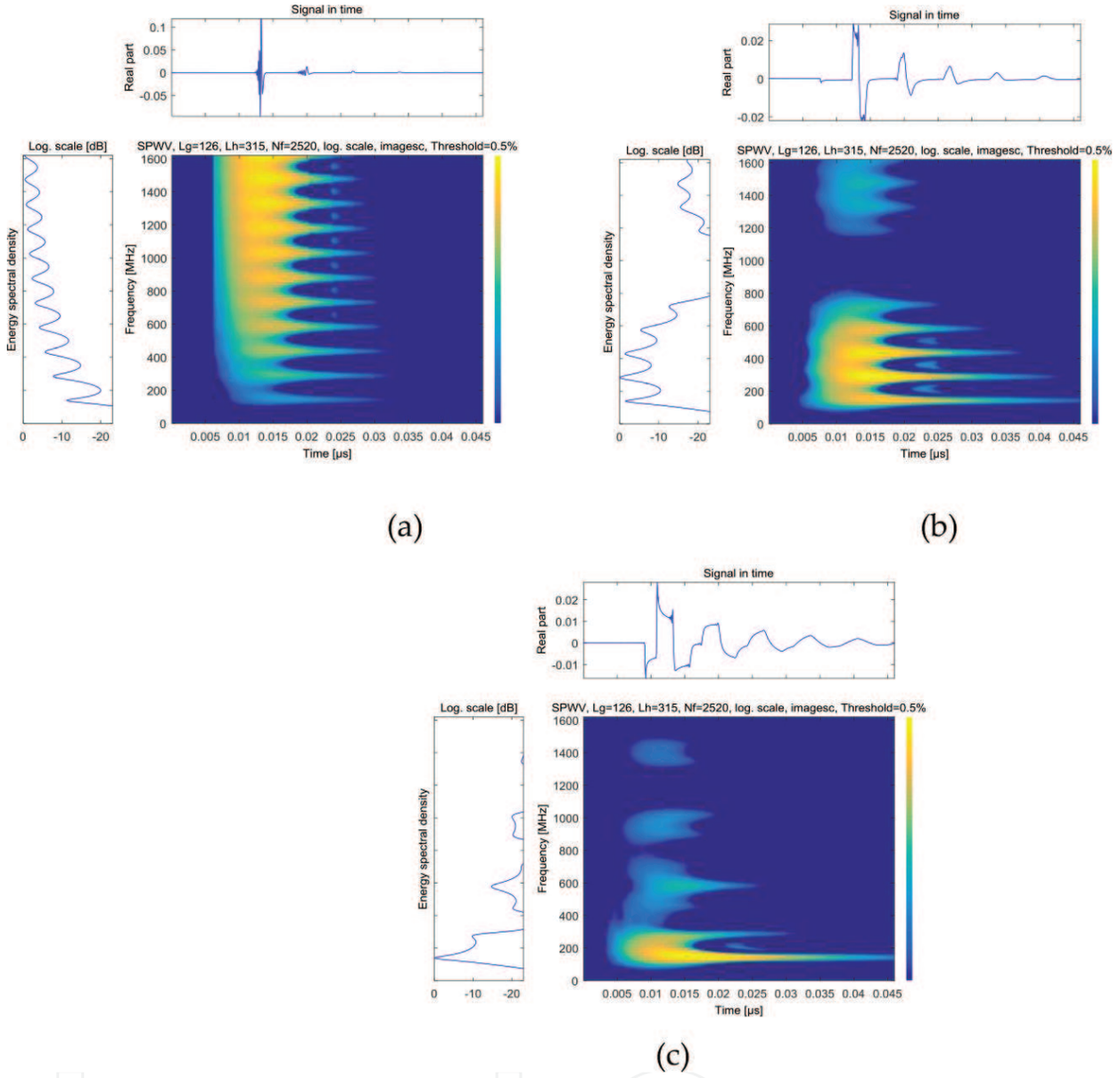

Figure 2. SPWVD of the wire scatterer with plane wave incidence at (a) $\theta = 15^{\circ}$, (b) $\theta = 45^{\circ}$, and (c)$\theta = 75^{\circ}$ (reprinted from [21] with permission from IEEE).

procedure, Rothwell [9–11] proposed that target recognition can be performed by convolving the target signatures with a special type of filter, known as the "extinction pulse" or the "E-pulse," in the time domain. The E-pulse is specially designed such that it will annul all the NRFs embedded in the late time response only if it is convolved with the response from the "true target." Mathematically, the E-pulse, $e(t)$, can be defined as [9–11]

$$c(t) = \int_0^{T_E} e(\tau) r(t-\tau) d\tau = 0 \quad \text{for} \quad t > T_L = T_l + T_E, \tag{5}$$

where $r(t)$ is the late time target signature defined in Eq. (2), T_l is the commencement of the late time period, and T_E is the duration of $e(t)$.

To illustrate how E-pulse operates, an ATR scenario is shown in **Figure 3** [11]. The goal here is to identify the target given a measured target signature $v(t)$ from an unknown target [11]. In the target library, a number of E-pulses corresponding to different targets are stored. To perform ATR, $v(t)$ is convolved with each of the E-pulses independently. According to Eq. (5), the one with a null response or smallest signal strength corresponds to the "true" target. Target identification is thus performed by monitoring the output of the convolution and picks up the one with the small energy level. To automate the process, the output is quantified using E-pulse discrimination number, *EDN*, and the E-pulse discrimination ratio, *EDR*, which are defined as follows [11]:

$$EDN = \left[\int_{T_L}^{T_L+W} (e(t)^* v(t))^2 dt\right]\left[\int_0^{T_e} e^2(t)dt\right]^{-1} \tag{6}$$

$$EDR = 10\log_{10}\left[\frac{EDN}{\min\{EDN\}}\right] \tag{7}$$

Therefore, the target signature yielding the smallest *EDN* and 0 dB *EDR* is the one corresponding to the target of interest. This forms the basis for E-pulse ATR.

In most of our studies, we know a priori which one is the "right" target, and our goal is to determine if E-pulse is capable of discriminating the targets in new applications; for instance, the "banded" E-pulse technique that better discriminates between similar targets [33], a novel technique for subsurface target detection [34], and ATR using polarimetric signatures (Section 3.1). **Figure 4** shows the flowchart of how we validate the E-pulse technique. For the case of three targets, there are three target signatures and three E-pulses, resulting in nine convolutions. Instead of using *EDN* and *EDR* in Eqs. (6) and (7), we modify them and introduce $EDN_{p,q}$ and discrimination ratio, $DR_{p,q}$, to quantify and convolution outcome and discrimination performance. They are given as follows [33, 35]:

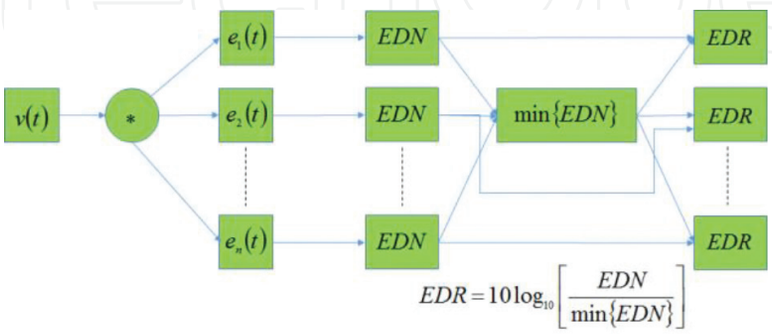

Figure 3. Automated target recognition using the E-pulse technique [11]. The goal is to determine which target does the unknown target signature $v(t)$ correspond to. $v(t)$ is convolved with all the E-pulses in the target library, and the corresponding EDN and EDR values are computed. the E-pulse that results in minimum value of EDN or equivalently 0 dB of EDR indicates the E-pulse "matches" with $v(t)$—The true target is thus the one that generate this E-pulse.

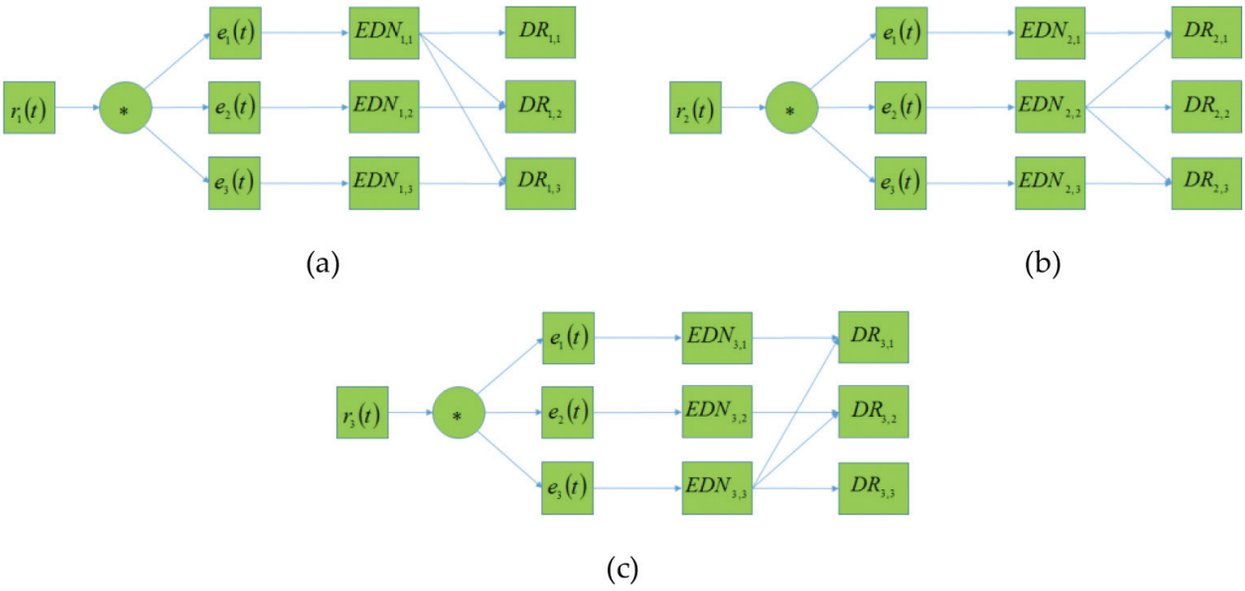

Figure 4. Validation of the E-pulse technique for new applications with known targets: (a) to (c) illustrate how the $EDN_{p,q}$ and $DR_{p,q}$ values are computed for the case of three known targets with target signatures ($r_1(t)$, $r_2(t)$, $r_3(t)$) and E-pulses ($e_1(t)$,$e_2(t)$,$e_3(t)$). As we know a priori of the "true" target, our goal is to test if we could obtain positive $DR_{p,q}$ ($p \neq q$) values.

$$EDN_{p,q} = \frac{\left[\int_{T_L}^{T_L+W} \left(e_q(t)^* r_p(t)\right)^2 dt\right]}{\left[\int_0^{T_e} e_q^2(t)dt\right]\left[\int_{T_L}^{T_L+W} r_p^2(t)dt\right]} \tag{8}$$

$$DR_{p,q} = 10\log_{10}\left[\frac{EDN_{p,q}}{EDN_{p,p}}\right] \tag{9}$$

$EDN_{p,p}$ is the case when the E-pulse and target response are from the same target, while $EDN_{p,q}$ is the case which the E-pulse and target returns are from different targets. A positive value of $DR_{p,q}$ implies that $EDN_{p,q}$ is greater than $EDN_{p,p}$ and thus a successful target recognition. As we have a priori knowledge of correct targets, positive $DR_{p,q}$ values are simply a validation of the success of E-pulse ATR or detection in the aforementioned new applications.

In practice, the E-pulse of a target can be obtained by numerically solving the convolution integral in Eq. (5) given the target signature [36] or using the formulation in [10] given the NRFs of the target. The E-pulses used in our studies (e.g., [33–35]) are constructed using the formulation in [10] together with the NRFs extracted from MPM.

3. Recent developments

Upon the introduction of SEM in the 1970s until the mid-1990s, research has mainly concentrated on three directions: theoretical studies with better modeling and description of early

time scattering phenomena [15–16], signal processing solutions to better retrieve SEM parameters for target characterization [17, 19–20, 36–39], and development of E-pulse and other ATR solutions for target recognition [11, 33, 40–44]. Most studies focused on ATR for targets in free space. The E-pulse proposed by Rothwell et al. [9–11, 36, 42] and the MPM algorithm by Sarkar and Pereira [20] have become the benchmark for filter-based ATR techniques and NRF extraction in this context. Since the 2000s, research activities have shifted toward applying the techniques developed in resonance-based target recognition for different applications. These include subsurface target detection, nondestructive evaluation, and medical diagnosis. Instead of using the linearly polarized electromagnetic wave to excite the target, the prospect of using fully polarimetric target signatures for ATR has also been investigated.

In this section, we first discuss the use of full polarimetric measurement and its impact on resonance-based target recognition. The merit of using polarimetric transient signatures is demonstrated through numerical examples. Then, different strategies for handling the *multiple-aspect multiple-polarization* data sets in multi-static scenarios are evaluated. Toward the end of the section, research activities on applying the E-pulse technique for different applications will be covered.

3.1. ATR using polarimetric signatures

The aspect dependency, as demonstrated in the above wire scattering example, as well as the polarization dependency of the residues, would limit the reliability and performance of ATR as it is uncertain whether all the dominant NRFs are well excited because the target orientation is usually not known a priori. In the mid-2000s, Shuley et al. [9] studied the residues retrieved from a target at 18 linear polarization angles at the same aspect and found that the residues of some NRFs could be so small at some polarization angles such that these NRFs are not retrieved. This was the first instance where polarization dependency of the residues is demonstrated. If we evaluate the RCS of the target at the resonant frequencies, the amplitudes of the scattered field, in general, vary as the observation aspects and polarization. This explains the aspect and polarization dependencies of the residues.

To accurately characterize a target using NRFs extracted from measured target signatures, it is important to incorporate more than one target signature obtained from different aspects and polarization states. Lui and Shuley [45] investigated different ways to process target signatures obtained from a number of polarization angles at a single aspect. Our results show that using the modified MPM [39] that allows extraction of one set of NRFs from multiple target signatures is preferred as it does not corrupt the original time-domain information and the risk of ignoring dominant modes is eliminated [45]. The major drawback is that the computational load grows as the number of target signatures (aspects and polarization angles) is increased. Also, when linear polarization is used, it is not trivial to decide how many polarization angles are sufficient. To better understand the impact of using the different polarimetric response for ATR, examples of some simple wire targets will first be presented. Then, different ways to handle data set obtained from *multiple-aspect multiple polarization* measurements for target classification will be presented.

http://dx.doi.org/10.5772/intechopen.75059

In polarimetry, the Sinclair scattering matrices [46] in the linear and circular polarization bases are given by

$$[S(H,V)] = \begin{bmatrix} S_{HH} & S_{HV} \\ S_{VH} & S_{VV} \end{bmatrix} \quad \text{and} \quad [S(L,R)] = \begin{bmatrix} S_{LL} & S_{LR} \\ S_{RL} & S_{RR} \end{bmatrix}. \tag{10}$$

Here, the subscripts denote the polarization channels (sets of transmit-receive polarization), where V, H, L, and R correspond to vertical, horizontal, left-hand, and right-hand circular polarization, respectively. The scattering matrices relate the incident and scattered electric field of the target under different polarization bases at a particular frequency. The first and second subscripts in each of the term inside the Sinclair scattering matrix correspond to the polarization state from the transmitting and receiving antennas. For instance, S_{VH} corresponds to the case where the target is illuminated using vertically polarized plane wave and the horizontally polarized scattered field is measured. Once the Sinclair scattering matrix is measured in an orthogonal basis, all the polarization states (linear, circular, and elliptical) can be synthesized such that it is not necessary to illuminate the target with a large number of linear polarization angles from the same aspect [9, 45]. Only four target signatures (three for monostatic) are required which considerably reduces the amount of data to be processed.

To investigate the impact of the excitation and receiving states to the performance of ATR, numerical examples of three wire targets shown in **Figure 5** were studied [47]. The targets are made up of two wire segments—a vertical wire segment (main body) of 1 m and a horizontal wire segment of 0.3 m (Target 1 and Target 3) and 0.2 m (Target 2) located at the center (Target 1 and Target 2) and at 0.2 m away from the end of the main body (Target 3), respectively. The scattering problems of these targets are solved in the frequency domain using FEKO [24] with 512 equally spaced frequency samples from 3.9 MHz to 2 GHz. The polarimetric transient signatures, or equivalently the scattering matrices in the time domain, i.e.,

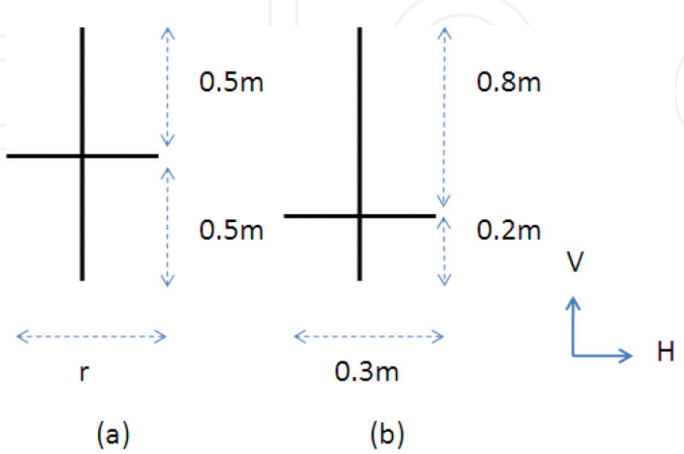

Figure 5. Wire targets and corresponding excitation polarization references. (a) Target 1: $r = 0.3m$, target 2: $r = 0.2m$, and (b) target 3 (reprinted from [47] with permission from IEEE).

$$\left[S_{(H,V)}(t)\right] = \begin{bmatrix} S_{HH}(t) & S_{HV}(t) \\ S_{VH}(t) & S_{VV}(t) \end{bmatrix} \quad \text{and} \quad \left[S_{(L,R)}(t)\right] = \begin{bmatrix} S_{LL}(t) & S_{LR}(t) \\ S_{RL}(t) & S_{RR}(t) \end{bmatrix}, \tag{11}$$

are determined using the aforementioned indirect time-domain method [22]. For each target, the NRFs from each target signature is extracted using MPM [20] resulting eight sets of NRFs and residues. At each polarization state, the E-pulses for each of the three targets (denoted as target q) are constructed using the extracted NRFs [10]. To evaluate the E-pulse ATR performance, the E-pulse validation procedures shown in **Figure 4** are applied. The E-pulse of each target (denoted as target q) is convolved with the target signatures from different targets (denoted as target p) but with the same polarization state. Before the convolution, both the E-pulses and target signatures are resampled as usually the sampling rate of the E-pulse and the target signatures are not the same [35]. The $EDN_{p,q}$ and $DR_{p,q}$ are computed, resulting in nine sets of $EDN_{p,q}$s and $DR_{p,q}$s for each polarization state. The corresponding results are tabulated in **Table 2**.

Under vertical excitation, the main body is excited but not the horizontal wire segment. Theoretically, the cross polarized response should be zero in this case and vice versa for horizontal polarization excitation, and thus we only consider the co-polarized components. As tabulated in **Table 2**, the E-pulse technique fails to recognize between Target 1 and Target 2 for the case of $S_{VV}(t)$, with $DR_{1,2}$ and $DR_{2,1}$ values near to 0 dB as only the NRFs corresponding to the main body are excited. For the case of $S_{HH}(t)$, the horizontal wire segments of the two targets are well excited, and $DR_{1,2}$ and $DR_{2,1}$ values of 46.6 and 126.2 dB are obtained, which indicates successful target recognition. However, almost 0 dB of $DR_{1,3}$ and $DR_{3,1}$ values result. This is because the length of the horizontal wire segment of Target 1 and Target 3 is identical and the transient responses are strongly dominated by the horizontal wire segments. Under vertical polarization, the current distributions of the two targets are different due to different positions of the horizontal wire segments. The $DR_{1,3}$ and $DR_{3,1}$ values of 42.9 and 65.4 dB

$DR_{p,q}$(dB)	(a) $S_{VV}(t)$			(b) $S_{HH}(t)$		
	$p = 1$	$p = 2$	$p = 3$	$p = 1$	$p = 2$	$p = 3$
$q = 1$	0	0.01	42.9	0	46.6	0.002
$q = 2$	−0.01	0	42.9	126.2	0	126.2
$q = 3$	65.4	65.4	0	−0.002	53.9	0
$DR_{p,q}$(dB)	(c) $S_{LL}(t)$			(d) $S_{LR}(t)$		
	$p = 1$	$p = 2$	$p = 3$	$p = 1$	$p = 2$	$p = 3$
$q = 1$	0	31.4	36.0	0	38.9	42.9
$q = 2$	27.0	0	43.8	26.7	0	44.6
$q = 3$	48.4	53.1	0	43.6	49.3	0

Table 2. ATR using target signatures under different polarization bases using E-pulse technique with the corresponding $DR_{p,q}$ (dB) values (reprinted from [47] with permission from IEEE).

result which indicate the E-pulses successfully distinguish between Target 1 and Target 3. With different positions and length of the horizontal wire segments, the E-pulse is capable of distinguishing between Target 2 and Target 3 for both $S_{VV}(t)$ and $S_{HH}(t)$. Under monostatic configuration and circularly polarized illumination, $S_{LL}(t) = S_{RR}(t)$ and $S_{LR}(t) = S_{RL}(t)$, and thus we only need to consider $S_{LL}(t)$ and $S_{LR}(t)$. $DR_{p,q}$values ($p \neq q$) of at least 26 dB result in all cases. Such results indicate that using circularly polarized target signatures can successfully discriminate the three targets.

In this example, ATR performance under different polarization states is studied. When the target is illuminated under linear polarization, only the main body or the horizontal wire segment is excited (details of the extracted NRFs can be found in [47]). The E-pulses are constructed using the incomplete set of NRFs. The target is poorly characterized and is not fully illuminated—these are the two main causes of the inconsistency in ATR performance. An example of the inconsistency in ATR performance due to aspect dependencies of the NRFs is reported in [48]. When the target is illuminated under circular polarization, the NRFs of both wire segments are adequately excited. The constructed E-pulse contains the domain NRFs of the entire target. The target is well characterized and well illuminated under circular polarization. The consistent ATR performance originates from the fact that the NRFs of both wire segments of the targets are well excited. The findings from this example demonstrated the importance of including all the dominant NRFs (including both the global and partial/substructure resonances [30]) for target classification, as well as the importance of exciting all the dominant NRFs, especially when a library of similar targets is considered [33].

3.2. Target classification using *multiple-aspect multiple-polarization* data set

Owing to the aspect and polarization dependencies of the residues, it is unlikely that the entire set of dominant NRFs can be excited from only one target signature. As shown above, target signatures obtained from different aspects and polarization states excite a different subset of dominant NRFs. Certainly, the use of multiple target signatures obtained from multiple aspect and polarization states for target characterization allows us to retrieve at least a larger subset of dominant NRFs within the frequency bandwidth. The *multiple-aspect multiple-polarization* data set [49], a data set that consists of transient target signatures obtained with different transmit-receive configurations and polarization basis, is thus required. There are a number of possible ways to illuminate the target and post-process these target signatures, and we want to identify an efficient way to handle the data. To illustrate the different possible ways to handle such large data sets, an example of a simple human breast model shown in **Figure 6 (a)** and **(b)**, a lossless dielectric hemisphere with a small different dielectric spheres embedded, that mimics the breast cancer detection scenario [50–53] is used. The radius of the lossless hemisphere is 60 mm with the relative permittivity of 5 (fat infiltrated tissue at ~3 GHz [54]). A 10 mm radius lossless dielectric sphere with a relative permittivity of 50 (taken from the Debye model [55] for <3 GHz) embedded inside the hemisphere is used to model the tumor. The target is illuminated using plane wave at six different aspects ($\theta = 105^\circ$ and $\phi = 30^\circ,\ 60^\circ,\ 90^\circ,\ 120^\circ,\ 150^\circ$ and 180°, where θ is measured from the positive z-axis, while

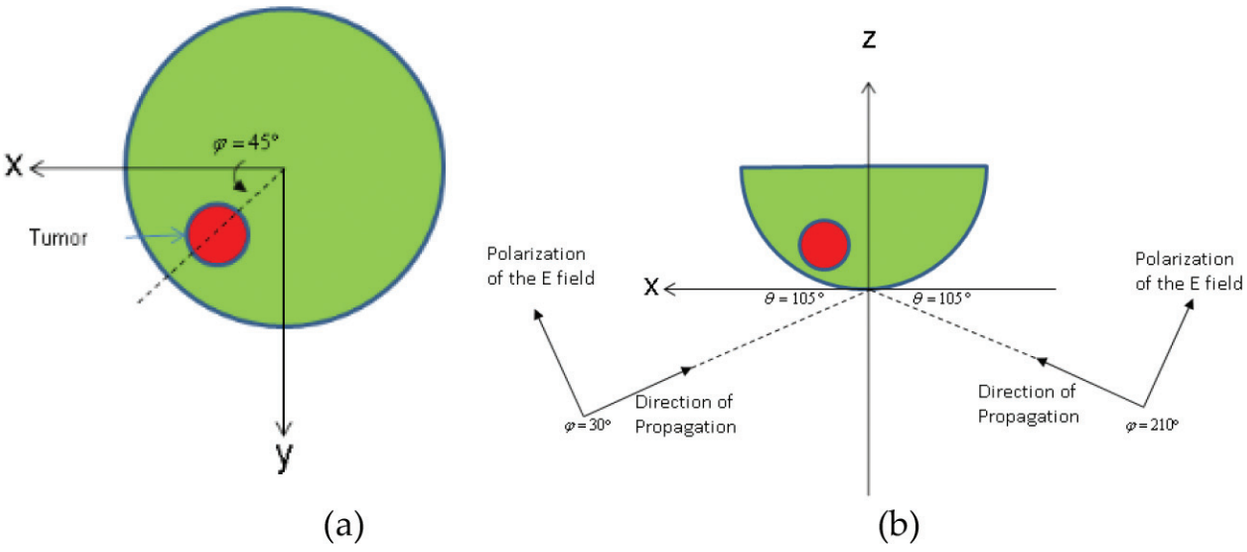

Figure 6. (a) Cross-sectional views (x-y plane) of the target. (b) Cross-sectional view ($\phi = 30^{\circ}, \theta = 105^{\circ}$) of the breast volume under plane wave illuminations from $\theta_t = 105^{\circ}$, $\phi_t = 30^{\circ}$, and $\phi_t = 210^{\circ}$, respectively. (reprinted from [49] with permission from IEEE).

ϕ is measured from the positive x-axis), resulted in 36 transmit-receive combinations (6 are monostatic, and 30 are bistatic) and 8 polarization states, i.e., 288 target signatures. It is apparent that the amount of data is tremendously increased when both aspect and polarization domains are considered. Efficient methods to handle the data are thus required.

First, extraction results of the entire *multiple-aspect multiple-polarization* data sets with 288 target signatures (Case 1: 6 × 6aspects and eight polarizations) are tabulated in column 2 of **Table 3**. Six dominant resonant modes are extracted. This result is treated as a *ground truth* as the extraction has taken all the data into account. Next, we consider NRF extractions in linear and circular polarization bases separately with 144 target signatures (Case 2: 36 aspects and four polarization states) in each basis. All the six resonant modes are retrieved in both bases, and the corresponding boxes in columns 3 and 4 in **Table 3** are shaded. The results indicate that both bases should give similar results in the NRF extraction process once all the four components in the Sinclair matrix are utilized.

Lastly, we perform NRF extraction on the multiple-aspect-only data at each of the eight polarization states (Case 3: 36 aspects and one polarization states). When *HH* data is used, five out of six resonant modes were extracted. When *VV*, *HV*, and *VH* data is used, only four modes were retrieved. When any one of the circularly polarized target signatures is used, all the six modes are accurately retrieved in all the co- and cross polarized results. The results show that we can retrieve all the dominant NRFs when only one of the four circularly polarized target signatures is used in the extraction process.

In summary, it is essential to include multiple-aspect data for target characterization because the NRF can be poorly excited at specific transmit-receive configurations [39, 48]. If all the four components in the scattering matrix are utilized for resonance extraction, both linear and circular polarization bases should give similar results. If only one out of the four components

Aspects	**Case 1 All (6 × 6)**	**Case 2 All (6 × 6)**		**Case 3 All (6 × 6)**							
Pol.	**Linear + circular (4 + 4)**	**Linear (4)**	**Circular (4)**	***VV***	***HH***	***HV***	***VH***	***LL***	***RR***	***RL***	***LR***
P	288	144	144	36	36	36	36	36	36	36	36
NRFs $\frac{\sigma \pm j\omega}{c}$	$-3.48 \pm j27.97^{1}$										
	$-4.52 \pm j32.93^{2}$										
	$-2.13 \pm j41.59^{3}$										
	$-3.14 \pm j45.27^{4}$										
	$-3.27 \pm j52.66^{5}$										
	$-4.16 \pm j57.63^{6}$										

The shaded boxes indicate the NRF is properly retrieved in the extraction process (***P***, total number of target signatures; Reprinted from [49] with permission from IEEE)

Table 3. Comparison of the extracted natural resonance frequencies (NRFs) using *multiple-aspect multiple-polarization* data.

in the polarization matrix is utilized (regardless single or multiple aspects), circularly polarized components are preferred over linearly polarized components as some of the dominant modes may not be retrieved in certain linear polarization states. Compared to previous studies that require a large number of target signatures from multiple linear polarization angles (6 [45] and 18 [9]), the computational load is reduced to the maximum of four or even one without deteriorating the accuracies of the extracted NRF when polarimetric signature is utilized to handle the polarization dependency of the residues. The findings presented here provide us with guidelines on how we should illuminate the targets and process the *multiple-aspect multiple-polarization* data set to extract a set of NRF that includes all the dominant NRFs for target characterization. With the "completed" set of NRF, the E-pulse is constructed and then used for ATR. In most ATR scenarios in which only one target signature from the target is measured, the traditional E-pulse technique using the "completed" E-pulse should be able to effectively distinguish the correct targets from the others. In situations, where more than one target signatures from a target are considered for ATR, e.g., the situation of multidirectional E-pulse presented in [48], novel ATR procedures will be required to effectively utilize the "completed" set of NRF with the extensive data set.

3.3. Subsurface target detection

Other than target recognition problems with the target in free space, research activities have also focused on subsurface target detection—where the target is located at a particular depth below an interface. The motivation of subsurface target detection first originated from unexploded ordinance (UXO) detection using ground-penetrating radar [56–60] and later detection of tumors inside a breast volume [49, 51, 55, 61] as well as detection of small changes in hip prostheses [62–64].

In the subsurface target detection problem, usually the excitation and the measured field points are located in one medium, and the target is located in another medium. The scattered response is no longer solely dependent on the target itself but also interactions between the target and the interface. These interactions vary as the dielectric contrast between the two media, the depth and the orientation of the target [56–60], as well as the interactions between the heterogeneity of the medium and the target. In [65], a transient scattering of metallic targets sited below lossless and lossy half space is studied using joint TF analysis. All the interactions of the target and the dielectric interface, as well as attenuation phenomena due to the non-zero conductivity of the half space, are clearly observed in the joint TF domain. Considering a relatively simple situation where both media are homogeneous, studies have demonstrated that there are two types of resonances associated with the entire scattering problem—a target resonance and an image resonance. A target resonance is the NRF associated with the target attributes (geometry and the dielectric properties) and the dielectric properties of the medium in which the target is embedded [56–60]. An image resonance is the NRF that corresponds to the target depth—the distance between the target and the interface of the two media [56, 57]. For target detection and recognition applications, the target NRF is of interest. Studies [56–58, 63] showed that the target NRFs forms a spiral trajectory in the S-plane as the target depth changes. The spiral trajectory surrounds the target NRF within a homogeneous environment—the case where the target is fully immersed in the environment without a dielectric interface.

Other than the characterization of the target resonances for the subsurface target, attempts have also been made to apply the E-pulse for monitoring depth changes [64, 66] and geometrical changes [67] of a hip prosthesis model sited below a half space of tissue. Results show that the E-pulse technique is capable of detecting both depth changes and physical changes of the target. A subsurface target detection technique is proposed in which the E-pulse is constructed using the NRFs for a target inside a homogenous environment [60] to approximate the target NRFs for subsurface targets. This E-pulse is convolved with target signatures from the subsurface target and shows that this approximate technique can distinguish between different targets [34, 68, 69].

3.4. Other applications

A critical issue that affects the accuracies of the extracted NRFs is the commencement of the late time or the turn-on time of the resonant modes [30]. The damped exponential model given by Eq. (2) is strictly only valid during the late time period. The early time consists of high-frequency scattering centers that are mainly local scattering events, which can be modeled using the entire functions (e.g., a Gaussian [17]). The inclusion of the early time period into the NRF extraction process will undoubtedly degrade the accuracies of the retrieved NRFs. Automated detection of the commencement of late time without a priori knowledge of the target geometry or orientation becomes crucial for ATR. Hargrave et al. [70] proposed a method to estimate the commencement of the late time based on intrinsic differences between the full-rank Hankel matrix generated from the early time data and the rank-deficient late time matrix generated by discrete resonant components. Rezaiesarlak and Manteghi [71, 72] propose the short-time matrix pencil method (STMPM), which mostly applies the MPM for NRF extraction

within a time window with a proper direction. The time window is moved by small time steps, and the extraction process is repeated until the entire signal is covered. The STMPM was first applied to chipless radio-frequency identification (RFID) application [71–74]. Data is encoded as NRFs of the RFID tagged by incorporating notches in the structure such that each RFID tag has different NRFs [73, 74].

In addition to the applications above, the concept of late time resonances has also been applied to sensing applications in other disciplines. This includes monitoring the deployment of arterial stents [75], nondestructive evaluation of the maturity of fruit [76], automated detection of objects fallen on railway tracks [77], nondestructive evaluation of layered materials [78, 79], and detection of concealed handguns [80].

4. Conclusions and ongoing challenges

The fundamentals and development of resonance-based target recognition over the last 40 years have been briefly reviewed. Prospects of using polarimetric transient signatures for target classification and recognition have been demonstrated through numerical examples. Results show that the use of polarimetric signatures will undoubtedly enhance the ATR performance while reducing the amount of data to process.

Other than using a linear polarization basis to synthesize the circularly polarized target signature, the challenges for designing circularly polarized time-domain antennas [81] that directly generate circularly polarized pulses are an ongoing research topic for antenna engineers. In situations where the targets under test are very similar, the resonance-based target recognition would perform poorly and probably fails. Recent results in [51, 82, 83] have shown that incorporating polarimetric features, e.g., characteristic polarization states (CPS) of the resonance modes, can solve the problem. Development of novel target recognition schemes that utilize these novel feature sets would be of practical interest to the radar community.

In addition to defense and security applications, recent studies have been looking into the potential of applying the technology to nondestructive evaluations, medical diagnosis, RFID, and agricultural applications. Compared to radar applications where the target is isolated (e.g., aircrafts in the sky) and located in the far-field region and direct signal path from transmitting and receiving antennas exists higher-order interactions between the targets and antennas as well as scattering from surrounding objects become significant especially when the target is located in the near-field region in medical diagnosis [52, 53] and aforementioned RFID applications. Novel calibration procedures [84, 85] and signal processing solutions for NRF extractions of multiple targets [86–88] are still ongoing research topics for researchers to explore. Regarding subsurface target detection, our results demonstrate that the E-pulse is capable of detecting changes of the NRFs of subsurface targets due to depth [64, 66] and geometrical changes [67]. In conjunction with target NRF, other features embedded in the target signature, such as the "turn-on" time of the resonance [65], could also be used for these applications. Rather than solely relies on NRF for ATR, the trend of having a "combined" feature set with

other parameters (e.g., CPS, turn-on time) will become the fashion for further development in this context.

Author details

Hoi-Shun Lui[1]*, Faisal Aldhubaib[2], Stuart Crozier[1] and Nicholas V. Shuley[1]

*Address all correspondence to: h.lui@uq.edu.au

1 School of Information Technology and Electrical Engineering, The University of Queensland, St. Lucia, Queensland, Australia

2 Electronics Department, College of Technological Studies, Public Authority for Applied Education, Kuwait

References

[1] Sullivan RJ. Radar Foundations for Imaging and Advanced Concepts. Raleigh: Scitech Publishing; 2004

[2] Knott EF, Shaeffer JF, Tuley MT. Radar Cross Section: Its Predication, Measurement and Reduction. Dedham, MA: Artech house; 1985

[3] Copeland JR. Radar target classification by polarization properties. Proceedings of the IRE. 1960;**48**:1290-1296

[4] Li HJ, Yang SH. Using range profiles as feature vectors to identify aerospace objects. IEEE Transactions on Antennas and Propagation. 1993;**41**:261-268

[5] Hurst M, Mittra R. Scattering center analysis via Prony's method. IEEE Transactions on Antennas and Propagation. 1987;**35**:986-988

[6] Lin H, Ksienski AA. Optimum frequencies for aircraft classification. IEEE Transactions on Aerospaces Electronic Systems. 1981;**17**:656-665

[7] Baum CE. The singularity expansion method. In: Felsen LB, editor. Transient Electromagnetic Fields. 1st ed. Vol. 10. Berlin; New York: Springer-Verlag; 1976. pp. 129-176

[8] Shuley N, Longstaff D. Role of polarisation in automatic target recognition using resonance descriptions. Electronics Letters. 2004;**40**:268-270

[9] Rothwell E, Nyquist D, Chen KM, Drachman B. Radar target discrimination using the extinction-pulse technique. IEEE Transactions on Antennas and Propagation. 1985;**33**:929-937

[10] Rothwell E, Chen KM, Nyquist DP, Sun W. Frequency domain E-pulse synthesis and target discrimination. IEEE Transactions on Antennas and Propagation. April, 1987;**35**(4): 426-434

[11] Ilavarasan P, Ross JE, Rothwell EJ, Chen KM, Nyquist DP. Performance of an automated radar target pulse discrimination scheme using E pulses and S pulses. IEEE Transactions on Antennas and Propagation. May, 1993;**41**(5):582-588

[12] Iwaszczuk K, Heiselberg H, Jepsen PU. Terahertz radar cross section measurements. Optics Express. 2010;**18**(25):26399-26408. DOI: 10.1364/OE.18.026399

[13] Lui HS, Taimre T, Lim YL, Bertling K, Dean P, Khanna SP, Lachab M, Valavanis A, Indjin D, Linfield EH, Davies AG, Rakic AD. Terahertz radar cross section characterization using self-mixing interferometry with a quantum Cascade laser. Electronics Letters. 22nd Oct. 2015;**51**(22):1774-1776

[14] Kennaugh EM, Moffatt DL. Transient and impulse response approximations. Proceedings of the IEEE. 1965;**53**:893-901

[15] Heyman E, Felsen L. A wavefront interpretation of the singularity expansion method. IEEE Transactions on Antennas and Propagation. 1985;**33**:706-718

[16] Felsen L. Comments on early time SEM. IEEE Transactions on Antennas and Propagation. 1985;**33**:118-119

[17] Jang S, Choi W, Sarkar TK, Salazar-Palma M, Kyungjung K, Baum CE. Exploiting early time response using the fractional Fourier transform for analyzing transient radar returns. IEEE Transactions on Antennas and Propagation. 2004;**52**:3109-3121

[18] Harrington R. Field computation by the moment method. 2nd ed. USA: IEEE Press; 1993

[19] Van Blaricum M, Mittra R. A technique for extracting the poles and residues of a system directly from its transient response. IEEE Transactions on Antennas and Propagation. 1975;**23**:777-781

[20] Sarkar TK, Pereira O. Using the matrix pencil method to estimate the parameters of a sum of complex exponentials. IEEE Antennas and Propagation Magazine. Feb, 1995;**37**(1):48-55

[21] Lui HS, Shuley N. On the analysis of electromagnetic transients from radar targets using smooth pseudo Wigner-Ville distribution (SPWVD). Proc. IEEE Antenna Propag. Society Int. Symp., pp. 5701-5704, Honolulu, HI, Jun. 10–15, 2007

[22] Lui HS, Shuley NV. On the modelling of transient scattering under ultra wideband sources. Asia Pacific Symp. Electromag. Compat., Beijing, China. 12–16 April 2010. pp. 854-857

[23] Rao SM. Time Domain Electromagnetics. San Diego: Academic Press; 1999

[24] FEKO, 32 Techno Lane, Technopark, Stellenbosch, 7600, South Africa: EM Software and System S.A., (pty) Ltd

[25] Rothwell EJ, Chen KM, Nyquist DP. Approximate natural response of an arbitrarily shaped thin wire Scatterer. IEEE Transactions on Antennas Propagation. Oct 1991;**39**(10): 1457-1462

[26] Cohen L. Time-Frequency Analysis. Englewood Cliffs, NJ: Prentice Hall; 1995

[27] Auger F, Flandrin P, Goncalves P, Lemoine O. Time-Frequency Toolbox – For Use with MATLAB. CNRS (France) and Rice University (USA; 1996)

[28] Lui HS, Shuley NV, Longstaff ID. Time-frequency analysis of late time electromagnetic transients from radar targets. Proc. IET Radar 2007, Pp. 1-5, the Edinburgh International Conference Centre, UK. 15–18 Oct., 2007

[29] Lui HS, Shuley NV. Joint time-frequency analysis on UWB radar signals. Proc. Int.l Conf. Signal Process. Comm. Sys., Gold Coast, Australia, 17–19 Dec. 2007

[30] Lui HS, Shuley NVZ. Evolutions of partial and global resonances in transient electromagnetic scattering. IEEE Antennas on Wireless Propagation Letters. 2008;**7**:435-439

[31] Tesche FM. On the analysis of scattering and antenna problems using the singularity expansion technique. IEEE Transactions on Antennas and Propagation. Jan., 1973;**21**(1): 53-62

[32] Van Blaricum M, Pearson L, Mittra R. An efficient scheme for radar target recognition based on the complex natural resonances of the target. IEEE Antennas and Propagation Society International Symposium. 1975;**13**:416-419

[33] Lui HS, Shuley NVZ. Radar target identification using a "banded" E-pulse technique. IEEE Transactions on Antennas and Propagation. Dec., 2006;**54**(12):3874-3881

[34] Lui HS, Shuley NVZ, Rakic AD. A novel, fast, approximate target detection technique for metallic target below a frequency dependent Lossy Halfspace. IEEE Transactions on Antennas and Propagation. May 2010;**58**(5):1699-1710

[35] Lui HS, Shuley NVZ. Sampling procedures in resonance based radar target identification. IEEE Transactions on Antennas and Propagation. May 2008;**56**(5):1487-1491

[36] Rothwell E, Kun-Mu C, Nyquist D. Extraction of the natural frequencies of a radar target from a measured response using E-pulse techniques. IEEE Transactions on Antennas and Propagation. 1987;**35**:715-720

[37] Gallego A, Medouri A, Carmen Carrion M. Estimation of number of natural resonances of transient signal using E-pulse technique. Electronics Letters. 1991;**27**:2253-2256

[38] Ruiz DP, Carrion MC, Gallego A, Medouri A. Parameter estimation of exponentially damped sinusoids using a higher order correlation-based approach. IEEE Transactions on Signal Processing. Nov. 1995;**43**(11):2665-2677

[39] Sarkar TK, Park S, Koh J, Rao SM. Application of the matrix pencil method for estimating the SEM (singularity expansion method) poles of source-free transient responses from multiple look directions. IEEE Transactions on Antennas and Propagation. April, 2000; **48**(4):612-618

[40] Kennaugh E. The K-pulse concept. IEEE Transactions on Antennas and Propagation. 1981;**29**:327-331

[41] Chen KM, Nyquist D, Rothwell E, Webb L, Drachman B. Radar target discrimination by convolution of radar return with extinction-pulses and single-mode extraction signals. IEEE Transactions on Antennas and Propagation. 1986;**34**:896-904

[42] Rothwell EJ, Chen KM. A hybrid E-pulse/least squares technique for natural resonance extraction. Proceedings of the IEEE. 1988;**76**:296-298

[43] Carrion MC, Gallego A, Porti J, Ruiz DP. Subsectional-polynomial E-pulse synthesis and application to radar target discrimination. IEEE Transactions on Antennas and Propagation. 1993;**41**:1204-1211

[44] Blanco D, Ruiz DP, Alameda E, Carrion MC. An asymptotically unbiased E-pulse-based scheme for radar target discrimination. IEEE Transactions on Antennas and Propagation. 2004;**52**:1348-1350

[45] Lui HS, Shuley N. Resonance Based Radar Target Detection with Multiple Polarisations. Proc. IEEE Antennas Propag. Soc. Int. Symp. USNC/URSI National Radio Science Meeting. 9–14 July, 2006, Albuquerque, New Mexico, USA. pp. 3259-3262

[46] Mott H. Remote Sensing with Polarimetric Radar. New Jersey: Wiley; 2007

[47] Lui HS, Shuley NVZ. Resonance based target recognition using ultra-wideband Polarimetric signatures. IEEE Transactions on Antennas and Propagation, New Jersey. August 2012;**60**(8):3985-3988

[48] Zhang H, Fan Z, Ding D, Chen R. Radar target recognition based on multi-directional E-pulse technique. IEEE Transactions on Antennas and Propagation. Nov. 2013;**61**(11):5838-5843

[49] Lui HS. Characterization of radar target using multiple transient responses. IEEE Antennas on Wireless Propagation Letters. Sept. 2015;**14**:1750-1753

[50] Lui HS, Fhager A, Persson M. On the forward scattering of microwave breast imaging. International Journal of Biomedical Imaging, 15 Pages. May 2012

[51] Lui HS, Fhager A, Yang J, Persson M. Characterization and detection of breast cancer using ultra wideband Polarimetric transients. European Conference on Antennas and Propagation. Gothenburg, Sweden, 8–11 April 2013. pp. 2909-2913

[52] Lui HS, Fhager A, Persson M. Preliminary Investigations of Three-Dimensional Microwave Tomography Using Different Data Sets. European Conference on Antennas and Propagation, Prague, Czech Republic. 26–30 March 2012

[53] Lui HS, Fhager A, Persson M. Antenna Configurations of Microwave Breast Imaging. Asia Pacific Microwave Conference, 5–8 Nov., 2013, Seoul, Korea

[54] Gabriel S, Lau RW, Gabriel C. The dielectric properties of biological tissues: III. Parametric models for the dielectric spectrum of tissues. Physics in Medicine and Biology. Nov. 1996;**41**(11):2271-2293

[55] Huo Y, Bansal R, Zhu Q. Modeling of noninvasive microwave characterization of breast tumors. IEEE Transactions on Biomedical Engineering. 2004;**51**:1089-1094

[56] Vitebskiy S, Carin L. Moment-method modeling of short-pulse scattering from and the resonances of a wire buried inside a lossy, dispersive half-space. IEEE Transactions on Antennas and Propagation. 1995;**43**:1303-1312

[57] Geng N, Jackson DR, Carin L. On the resonances of a dielectric BOR buried in a dispersive layered medium. IEEE Transactions on Antennas and Propagation. 1999;**47**:1305-1313

[58] Wang Y, Longstaff ID, Leat CJ, Shuley NV. Complex natural resonances of conducting planar objects buried in a dielectric half-space. IEEE Transactions on Geoscience Remote Sensing. 2001;**39**:1183-1189

[59] Chen C-C, Peters L Jr. Buried unexploded ordnance identification via complex natural resonances. IEEE Transactions on Antennas and Propagation. 1997;**45**:1645-1654

[60] Baum CE. Detection and Identification of Visually Obscured Targets. Philadelphia: Taylor & Francis; 1999

[61] Lui HS, Li BK, Shuley N, Crozier S. Preliminary Investigation of Breast Tumor Detection Using the E-Pulse Technique. Proc. IEEE Antenna Propag. Soc. Int. Symp. USNC/URSI National Radio Science Meeting, pp. 283-286, 9–14 July. 2006. Albuquerque, New Mexico, USA

[62] Lui HS, Shuley N, Crozier S. A Concept for Hip Prosthesis Identification Using Ultra Wideband Radar. Proc. 26th Annual Int. Conf. of the IEEE Engineering in Medicine and Biology Society. pp. 1439-1442, 1–5 Sept. 2004, San Francisco, CA, USA

[63] Lui HS, Shuley N, Crozier S. Hip Prosthesis Detection Based on Complex Natural Resonances. Proc. 27th Annual Int.l Conf. of the IEEE Engineering in Medicine and Biology Society, 1–5 Sept. 2005. Shanghai, China. pp. 1571-1574

[64] Lui HS, Shuley N, Padhi SK, Crozier S. Detection of hip prosthesis depth changes using an E-pulse technique. Topical Meeting on Biomedical Electromagnetics. 17th International Zurich Symposium on Electromagnetic Compatibility. 27 February to 3 march 2006, Singapore. pp. 81-84

[65] Lui HS, Shuley N, Persson M. Joint time-frequency analysis of transient electromagnetic scattering from a subsurface target. IEEE Antennas and Propagation Magazine. Oct. 2012; **54**(5):109-130

[66] Lui HS, Shuley NVZ. Detection of depth changes of a metallic target buried inside a Lossy Halfspace using the E-pulse technique. IEEE Transactions on Electromagnetic Compatibility. November 2007;**49**(4):868-875

[67] Lui HS, Aldhubaib F, Shuley NVZ, Hui HT. Subsurface target recognition based on transient electromagnetic scattering. IEEE Transactions on Antennas and Propagation. October 2009;**57**(10):3398-3401

[68] Lui HS, Shuley N. Subsurface target recognition using an approximated method. Asia Pacific Microw. Conf. Singapore, 7–10 Dec. 2009. pp. 2216-2219

[69] Lui HS, Shuley NV. Performance evaluation of subsurface target recognition based on ultra-wideband short pulse excitation. IEEE Int. Symp. Antennas Propag., pp. 1-4, Toronto, Ontario, Canada, July 11–17, 2010

[70] Hargrave CO, Clarkson IVL, Lui HS. Late-time estimation for resonance-based radar target identification. IEEE Transactions on Antennas and Propagation. Nov., 2014;**62**(11): 5865-5871

[71] Rezaiesarlak R, Manteghi M. Short-time matrix pencil method for Chipless RFID detection applications. IEEE Transactions on Antennas Propagation. May 2013;**61**(5):2801-2806

[72] Rezaiesarlak R, Manteghi M. On the application of short-time matrix pencil method for wideband scattering from resonant structures. IEEE Transactions on Antennas Propagation. Jan. 2015;**63**(1):328-335

[73] Blischak AT, Manteghi M. Embedded singularity Chipless RFID tags. IEEE Transactions on Antennas Propagation. Nov 2011;**59**(11):3961-3968

[74] Rezaiesarlak R, Manteghi M. Complex-natural-resonance-based Design of Chipless RFID tag for high-density data. IEEE Transactions on Antennas Propagation. Feb 2014;**62**(2): 898-904

[75] Manteghi M, Cooperand DB, Vlachos PP. Application of singularity expansion method for monitoring the deployment of arterial stents. Microwave and Optical Technology Letters. 2012;**54**(10):2241-2246

[76] Tantisopharak T, Moon H, Youryon P, Bunya-Athichart K, Krairiksh M, Sarkar TK. Nondestructive determination of the maturity of the durian fruit in the frequency domain using the change in the natural frequency. IEEE Transactions on Antennas Propagation. Feb 2016;**64**(5):1779-1787

[77] Mroué A, Heddebaut M, Elbahhar F, Rivenq A, Rouvaen J-M. Automatic radar target recognition of objects falling on railway tracks. Measurement Science and Technology. Jan. 2012;**23**(2). DOI: 10.1088/0957-0233/23/2/025401

[78] Stenholm G, Rothwell EJ, Nyquist DP, Kempel LC, Frasch LL. E-pulse diagnostics of simple layered materials. IEEE Transactions on Antennas and Propagation. Dec. 2003; **51**(12):3221-3227

[79] Wierzba JF, Rothwell EJ. E-pulse diagnostics of curved coated conductors with varying thickness and curvature. IEEE Transactions on Antennas and Propagation. September 2006;**54**(9):2672-2676

[80] Harmer SW, Andrews DA, Rezgui ND, Bowring NJ. Detection of handguns by their complex natural resonant frequencies. IET Microwaves, Antennas and Propagation. 2010, 2010;**4**(9):1182-1190. DOI: 10.1049/iet-map.2009.0382

[81] Shlivinski A. Time domain circularly polarized antenna. IEEE Transactions on Antennas and Propagation. June 2009;**57**(6):1606-1611

[82] Aldhubaib F, Shuley NVZ, Lui HS. Characteristic polarization states in an ultra-wideband context based on singularity expansion method. IEEE Geoscience and Remote Sensing Letters. Oct. 2009;**6**(4):792-796

[83] Lui HS, Persson M. Characterization of radar targets based on ultra wideband Polarimetric transient signatures. XXX URSI General Assembly and Scientific Symposium of International Union of Radio Science. pp. 1-4. Istanbul, Turkey. 13–20 Aug. 2011

[84] Sarkar TK, Tseng FI, Rao SM, Dianat SA, Hollmann BZ. Deconvolution of impulse response from time-limited input and output: Theory and experiment. IEEE Transactions on Instrumentation and Measurement. 1985;**34**:541-546

[85] Bannawata L, Boonpoongaa A, Burintramartb S, Akkaraekthalina P. On the resolution improvement of radar target identification with filtering antenna effects. International Journal of Antennas Propagation. accepted for publication, Dec 2017

[86] Rezaiesarlak R, Manteghi M. A space–time–frequency Anticollision algorithm for identifying chipless RFID. IEEE Transactions on Antennas Propagation. Mar 2014;**62**(3):1425-1432

[87] Lee W, Sarkar TK, Moon H, Salazar-Palma M. Identification of multiple objects using their natural resonant frequencies. IEEE Antennas and Wireless Propagation Letters. 2013;**12**:54-57

[88] Lee JH, Jeong SH, Park GS, Lee YC, Cho SW. Performance analysis of natural frequency-based multiple radar target recognition for multiple-input–multiple-output radar application. IET Radar, Sonar and Navigation. June 2014;**8**(5):457-464

IntechOpen